The 2010 IEEE/RSJ International Conference on
Intelligent Robots and Systems
October 18-22, 2010, Taipei, Taiwan

Teleoperation of a Tail-Sitter VTOL UAV

Ren Suzuki, Takaaki Matsumoto, Atsushi Konno, Yuta Hoshino,
Kenta Go, Atsushi Oosedo and Masaru Uchiyama

***Abstract*— Vertical take-off and landing unmanned aerial vehicles (VTOL UAVs) are expected to perform dangerous mission such as rescue and exploring disaster site alone. As for the operation of a UAV in a rescue mission, teleoperation is preferred. This paper describes teleoperation of a miniature tail-sitter VTOL UAV. A teleoperation system is developed to navigate a tail-sitter UAV. A velocity estimation method for outdoor flight is described and a velocity control strategy based on attitude control for indoor hovering of tail-sitter VTOL UAVs is proposed. In order to verify the teleoperation system and velocity control strategy, indoor exploration and target tracking teleoperation are performed in this paper. Through the experiments, the operator successfully controlled a teleoperated tail-sitter VTOL UAV with non-line-of-sight. In addition, a preliminary obstacle avoidance system is also implemented to assist operator.**

I. INTRODUCTION

Tail-sitter VTOL UAVs are more efficient for rescue missions. Neither the fixed-wing UAVs nor the rotary-wing UAVs are capable of completing the rescue missions alone. It is difficult for fixed UAVs to fly indoors. And rotary-wing UAV is not proper for flying with long distance. VTOL UAVs are capable of both flying with long distance and hovering. The simplest way to perform VTOL maneuver is tail-sitting since it does not need extra actuators. Because a tail-sitter VTOL UAVs are simple mechanism and have features of both a fixed-wing UAV and a rotary-wing UAV, they can complete both of the missions (Fig. 1).

As for the operation of a UAV in a rescue mission, teleoperation is preferred, since completely autonomous UAV still has many problems for practical use, such as localization and path-planning. In addition, there are still some safety issues needed to be considered for an autonomous UAV. Human is superior in situational awareness and estimation. Therefore, teleopearated UAVs are suitable for rescue mission.

There are some researches about teleoperation of UAV. Beard et al. succeeded in teleoperation fixed-wing UAV [1]. Using PDA, the operator controlled the altitude, azimuth angle and velocity of UAV easily. However, the operator had a good direct view of aircraft. The aircraft performed only level flight, and indoor flight teleoperation was not discussed. Guenhard et al. practiced indoor hovering of four rotors VTOL vehicle [2]. The operator controlled UAV attitude and altitude by use of joystick. However, their system have not intended to fly where the operator could not watch the UAV directly.

This work was supported by Grant-in-Aid for Exploratory Research (No. 21656219), and JSPS Fellows (No. 216015).

Ren Suzuki, Takaaki Matsumoto, Yuta Hoshino, Atsushi Konno, Kenta Go, Atsushi Oosedo and Masaru Uchiyama are with Department of Aerospace Engineering, Tohoku University, Aoba-yama 6-6-01, Sendai 980-8579, Japan. takaaki@space.mech.tohoku.ac.jp

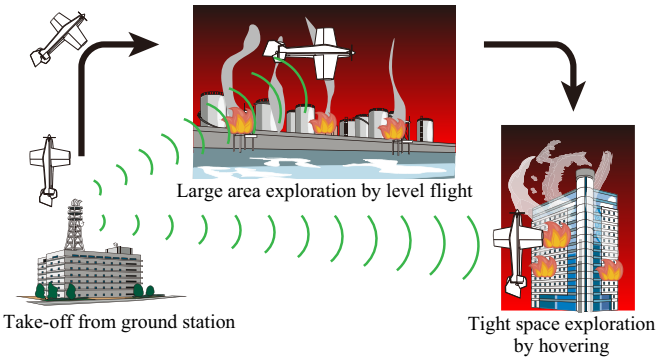

Fig. 1. Rescue mission of a tail-sitter VTOL UAV.

From the aspect of tail-sitter VTOL UAVs, only little attempt has been done to perform teleoperated flight. Stone et al. developed tail-sitter VTOL UAV called “T-wing” which has a canard wing and tandem rotors [3]. They proposed the control and guidance architecture and performed outdoor hovering experiment. However, the operator could watch the aircraft directly. Green et al. developed a simple tail-sitter VTOL UAV which airframe is single propeller R/C airplane [4]. They are proposed obstacle avoidance system to fly narrow space such as forests, caves and tunnels [5]. But their UAV was fully autonomous and teleoperated flight was not reported.

This paper describes teleoperation of a miniature tail-sitter VTOL UAV. A teleoperation system is developed to navigate a tail-sitter UAV. A velocity estimation method for outdoor flight is described and a velocity control strategy based on attitude control for indoor hovering of tail-sitter VTOL UAVs is proposed. In order to verify the teleoperation system and velocity control strategy, indoor exploration experiment and target tracking teleoperation without the line-of-sight of the operator are performed in this paper. Through the experiments, operator successfully navigated the tail-sitter VTOL UAV with non-line-of-sight. In addition, a preliminary obstacle avoidance system is also implemented to assist operator.

II. SYSTEM CONFIGURATION

A. Airframe

A tail-sitter VTOL UAV was developed [6],[7]. Overview of this UAV is shown in Fig. 2. The main wingspan is 1.0 m, and the weight is 0.75 kg. The main wing and tail wings are parts of a commercial R/C UAV (Hyperion Co.

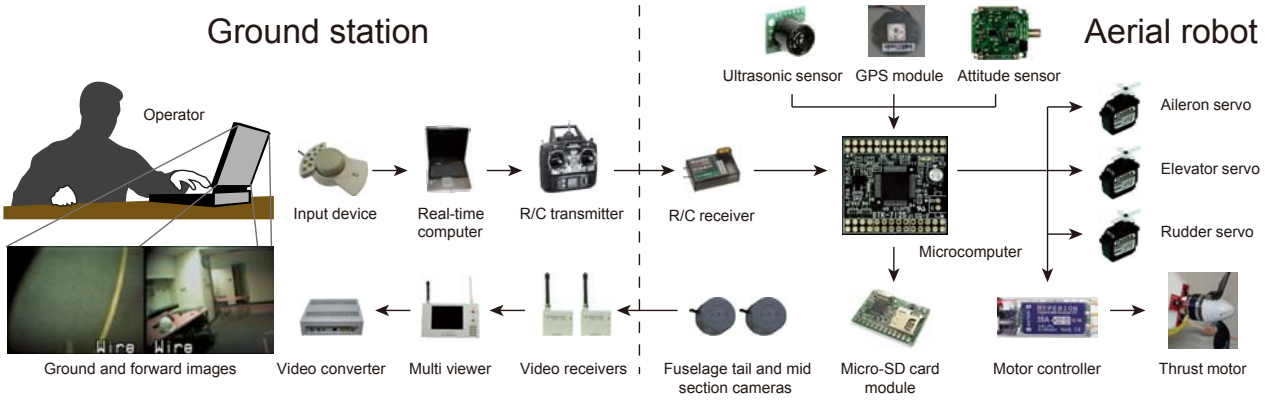

Fig. 3. Teleoperation system configuration.

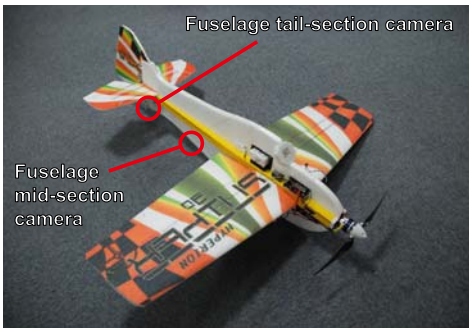

Fig. 2. Tail-sitter UAV.

Model SNIPER 3D). The body is newly developed. The UAV is controlled by mounted devices. This aircraft has a microcomputer and 3 sensors; a AHRS (Attitude Heading Reference Systems), a GPS (Global Positioning System) and an ultrasonic sensor. The GPS measures global position and ground speed. The AHRS measures attitude and acceleration. The ultrasonic sensor measures altitude from ground.

B. Teleoperation System

A teleoperation system for tail-sitter VTOL UAV was developed. Because tail-sitter VTOL UAVs have two flight modes; hovering and level flight, the teleoperation system must be able to deal with both two modes. The teleoperation system consists of following devices:

- **Fuselage tail-section camera**
  In order to investigate damage and find victim in hovering, the operator need to see the ground. The UAV is equipped with the fuselage tail-section camera.
- **Fuselage mid-section camera**
  The operator can hardly pilot the hovering UAV without the video of environment. To see foreground of the UAV, an another wireless camera is mounted on fuselage mid-section. This camera is also used for seeing ground during level flight.
- **Video receiver and converter**
  The wireless cameras send ground and front area views to ground station. The received radio wave of videos are integrated by the multi viewer.
- **6-degree-of-freedom input device**
  Seeing ground and forward views shown on computer, the operator controls the UAV through input device. Using 6 DOF input device (3D connexion Co. SpaceMouse) , the operator can pilot the UAV intuitively.
- **Control computer and transmitter**
  The control computer with real-time operating system converts input device control commands to pulse width modulated (PWM) signals. The PWM signal are sent by RC transmitter.

Fig. 3 shows a configuration diagram of the system.

C. Attitude Control

Each three axes of the UAV are controlled by a simple PID controller. The control command is sent to control surfaces corresponding to each axis as follows:

$$\delta_i = -\left(K_P w_i + K_I \int w_i dt + K_D \dot{w}_i\right), \qquad (1)$$

where δ_1, δ_2 and δ_3 are the aileron angle, elevator angle and rudder angle, respectively, and w_1, w_2 and w_3 are X, Y and Z components of axis-angle error between reference and current attitudes. The axis-angle error is calculated by a attitude transition strategy for a tail-sitter VTOL UAV that increases stability against large attitude disturbance [8]. The PID gains are determined by the ultimate sensitivity method, and tuned by trial and error. The attitude is operated by blowing a slip stream of the propeller to each control surface.

D. Altitude Control

The altitude controller is independently designed [6]. The desired propeller reference rotation speed is calculated from the reference and current altitudes. A feedback control of propeller rotation speed is developed to enhance robustness against battery condition and motor load changes.

III. TELEOPERATED HOVERING

A. Velocity Feedback Control for Outdoor Hovering

There are wind disturbances at outdoor environment, hence velocity feedback control is needed to perform fix-point hovering observation. Velocity measurement by GPS has few drift, but slower than control frequency. On the other hand, acceleration measurement by AHRS is fast, but has too large drift to integrate.

However, integrating GPS and AHRS through Kalman filter, fast, precise and stable velocity estimation can be realized [9]. It is divided into two stages; process update and measurement update. In order to implement Kalman filter, the state $\boldsymbol{x}$ and input $\boldsymbol{u}$ are defined as follows:

$$\boldsymbol{x} \equiv \begin{bmatrix} \boldsymbol{v}_o \\ h \end{bmatrix}, \quad \boldsymbol{u} \equiv \begin{bmatrix} \boldsymbol{a}_o \\ g \end{bmatrix},$$

where $\boldsymbol{v}_o$ is the UAV velocity vector with respect to the world coordinates, $\boldsymbol{a}_o$ is the UAV acceleration vector measured by AHRS with respect to the world coordinates, h is the UAV altitude and g is the gravity acceleration. The altitude is estimated at the same time, because it is important information to flight and measurable by GPS easily.

1) Process Update: Process update stage is performed as time passes. The estimated state $\widehat{\boldsymbol{x}}$ is updated as follows:

$$\begin{aligned} \widehat{\boldsymbol{x}}_k &= \widehat{\boldsymbol{x}}_{k-1} + \Delta\widehat{\boldsymbol{x}}_k \\ &= (\boldsymbol{I} + \boldsymbol{A}\Delta t)\widehat{\boldsymbol{x}}_{k-1} + \boldsymbol{B}\Delta t \boldsymbol{u}_{k-1}. \end{aligned} \tag{2}$$

where $\boldsymbol{I}$ is a 4×4 identity matrix and the matrices $\boldsymbol{A}$ and $\boldsymbol{B}$ are defined as follows:

$$\boldsymbol{A} \equiv \begin{bmatrix} 0 & 0 & 0 & 0 \\ 0 & 0 & 0 & 0 \\ 0 & 0 & 0 & 0 \\ 0 & 0 & 1 & 0 \end{bmatrix}, \quad \boldsymbol{B} \equiv \begin{bmatrix} 1 & 0 & 0 & 0 \\ 0 & 1 & 0 & 0 \\ 0 & 0 & 1 & -1 \\ 0 & 0 & \Delta t & -\Delta t \end{bmatrix}.$$

The covariance of the state $\boldsymbol{P}$ is updated as follows:

$$\boldsymbol{P}_k = (\boldsymbol{I} + \boldsymbol{A}\Delta t)\boldsymbol{P}_{k-1}(\boldsymbol{I} + \boldsymbol{A}\Delta t)^T + (\boldsymbol{B}\Delta t)\boldsymbol{Q}(\boldsymbol{B}\Delta t)^T, \tag{3}$$

where $\boldsymbol{Q}$ is the input error covariance, i.e,

$$\boldsymbol{Q} \equiv E\left[\boldsymbol{u}(\boldsymbol{u})^T\right].$$

2) Measurement Update: The measurement update stage is performed when the GPS outputs observed velocity and altitude $z \equiv \begin{bmatrix} \boldsymbol{v}_{GPS} & h_{GPS} \end{bmatrix}^T$.

The observation equation is following:

$$z = \boldsymbol{H}\boldsymbol{x} + \boldsymbol{v}, \tag{4}$$

where $\boldsymbol{H}$ is a 4×4 identity matrix and $\boldsymbol{v}$ is the measurement error of GPS.

Then, $\widehat{\boldsymbol{x}}$ and $\boldsymbol{P}$ are renewed by following equations:

$$\boldsymbol{K}_k = \boldsymbol{P}_k\boldsymbol{H}^T(\boldsymbol{H}\boldsymbol{P}_k\boldsymbol{H}^T + \boldsymbol{R})^{-1}, \tag{5}$$

$$\boldsymbol{P}_k \leftarrow (\boldsymbol{I} - \boldsymbol{K}_k\boldsymbol{H})\boldsymbol{P}_k, \tag{6}$$

$$\widehat{\boldsymbol{x}}_k \leftarrow \widehat{\boldsymbol{x}}_k + \boldsymbol{K}_k(z_k - \boldsymbol{H}\widehat{\boldsymbol{x}}_k)^{-1}, \tag{7}$$

where $\boldsymbol{K}$ is the Kalman gain and $\boldsymbol{R}$ is the observation error covariance, i.e.,

$$\boldsymbol{R} \equiv E\left[\boldsymbol{v}(\boldsymbol{v})^T\right].$$

3) Translational Velocity Estimation: Fig. 4 shows stationary state velocity and suggests validity of the Kalman filter. The translational velocity by AHRS integration was unstable and the velocity by GPS had impulsive noise, however the estimated velocity kept approx zero.

By using the Kalman filter, the velocity change of a UAV is estimated stably. Fig. 5 shows velocity change during stable vertical hover. In the experiment, the estimated velocity was stable and almost zero.

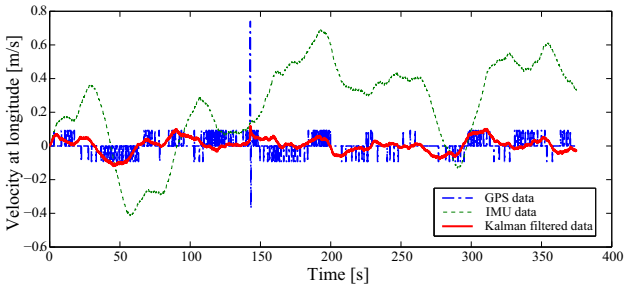

Fig. 4. Velocity estimation of stationary UAV.

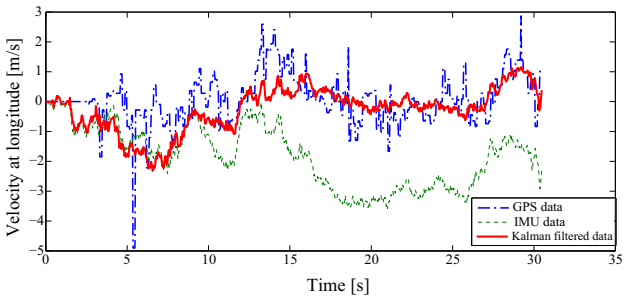

Fig. 5. Velocity estimation of hovering UAV.

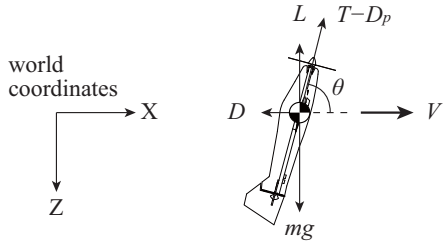

Fig. 6. Mathematical model and coordinates of hovering UAV.

B. Attitude Based Velocity Control for Indoor Hovering

The UAV can not receive GPS signal at indoor environment, and the Kalman filter can not work. However, there are few wind disturbances and attitude is still measurable precisely. There is a consistent relation between UAV attitude and its translational velocity in the steady state, hence the translational velocity can be controlled by attitude manipulation.

When the hovering UAV is in uniform motion which has only horizontal velocity (Fig. 6), its dynamic equations are following:

$$(T - D_p)\cos\theta - D = 0, \tag{8}$$

$$-(T - D_p)\sin\theta - L + mg = 0, \tag{9}$$

where T is the thrust force, D_p is the propeller drag force, θ is the pitch angle, D is the drag force, L is the lift force, m is the UAV weight and g is the gravity acceleration. Equations (8) and (9) are the equilibrium of horizontal and vertical forces, respectively. Substituting (9) into (8), the relation between pitch angle and horizontal forces is given as follows:

$$D\frac{\sin\theta}{\cos\theta} = mg - L. \tag{10}$$

Since the lift force L and the drag force D are aerodynamic forces, (10) can be rewritten as follows:

$$\frac{1}{2}\rho V^2 S C_D(\theta)\frac{\sin\theta}{\cos\theta} = mg - \frac{1}{2}\rho V^2 S C_L(\theta), \tag{11}$$

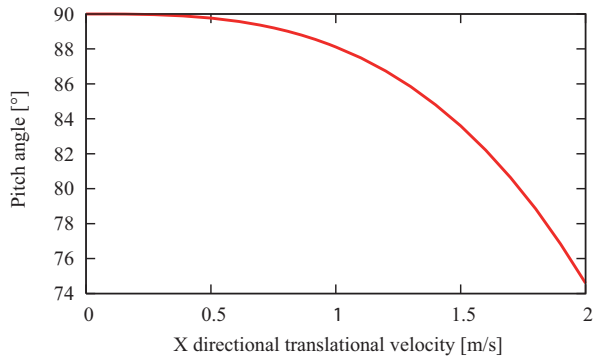

Fig. 7. The relation between pitch angle and X directional velocity.

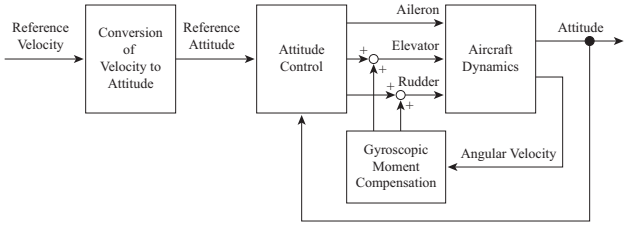

Fig. 8. Attitude based velocity control.

where ρ is the air density, S is the main-wings area, C_L and C_D are the lift and drag coefficients, respectively. V is the UAV translational velocity with respect to the world coordinates. When pitch angle θ is almost 90 ° , nonlinear variables of (11) are approximated as follows:

$$\sin\theta \approx 1 \ , \qquad \cos\theta \approx \frac{\pi}{2} - \theta \ ,$$
$$C_L(\theta) \approx A_{C_L}\theta + B_{C_L} \ , \quad C_D(\theta) \approx C'_D \ .$$

Finally, the relation between UAV pitch angle and horizontal velocity is given by,

$$\frac{1}{2}\rho V^2 S C'_D \frac{1}{\frac{\pi}{2} - \theta} = mg - \frac{1}{2}\rho V^2 S (A_{C_L}\theta + B_{C_L}) \ . \qquad (12)$$

Equation (12) can be solved easily (Fig. 7). Lateral relation between attitude and velocity are also solved. Therefore, utilizing these results, the translational velocity of indoor hovering UAV can be controlled. Fig. 8 is the block diagram of the control system. When operator inputs reference velocity by use of input device, reference attitude are calculated and attitude feedback control are executed. Becase the coordinates of the input device corresponds to the aircraft body coordinates (Fig. 9), operator can navigate the UAV with feeling of the reality that he is on-board.

C. Indoor Exploration Experiment

The teleoperated UAV explore partially destroyed building. Because most of casualties are on the floor, the operator must search ground from wall to wall. In order to verify the ground searching ability, teleoperated indoor exploration experiment was performed.

Fig. 10 shows the schematic view of indoor exploration experiment. The exploration space is rectangular area (2.5 m by 3.0 m). Since there is a partition wall between the UAV and the operator, the operator can not see the UAV and target at all. Viewing image of the fuselage tail-section camera, the

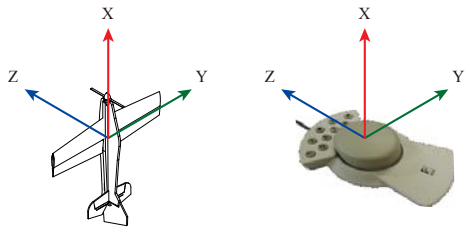

Fig. 9. Correspondence of hovering UAV and input device coordinates.

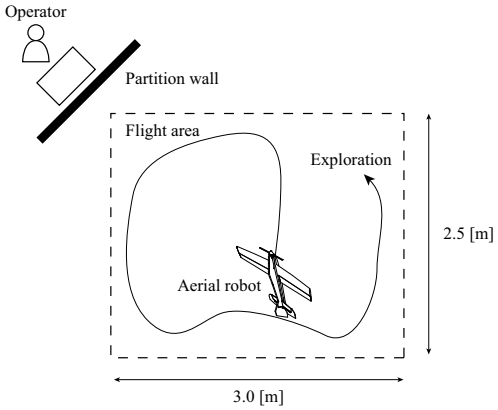

Fig. 10. Schematic view of indoor exploration experiment.

operator control the UAV position within the flight area. The UAV keeps constant altitude by feedback control.

The result of the experiment is shown in Fig. 11. The operator succeeded in the navigation of the UAV thoroughly without line-of-sight. The ground view was useful information (Fig. 12). The attitude change during experiment is shown in Fig. 13.

D. Target Tracking Teleoperation

There are many moving targets in observation area, and operators sometimes need to track some of them. The fuselage mid-section camera of UAV make this mission possible. To verify moving target surveillance ability, teleoperated target tracking was practiced.

Fig. 14 shows the schematic view of target tracking teleoperation. The target person walks in slow circles around the UAV. The operator pilots the UAV direction toward the target by use of input device and images of the fuselage mid-section camera.

The experiment result is shown in Fig. 15. The operator commanded the rotational velocity of UAV direction by use of Space Mouse. Utilizing fuselage mid-section camera, the operator successfully navigated the UAV direction toward the human target (Fig. 16).

IV. OBSTACLE AVOIDANCE

The operator should concentrate on move and surveillance. However, there are many obstacles at indoor environment and low altitude of disaster site, and the operator must avoid collision manually. Since there are control and communication delays, the operator has to employ “move and wait” strategy in general. But this strategy is inefficient and can not work against moving obstacle.

Fig. 11. Indoor exploration experiment.

Fig. 12. Indoor exploration experiment (fuselage tail-section camera).

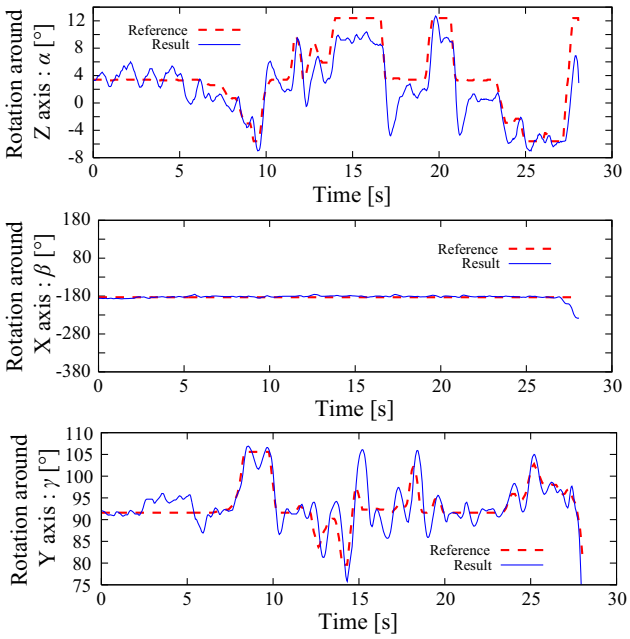

Fig. 13. Attitude change during indoor exploration experiment (α, β and γ are ZXY Euler angles, respectively).

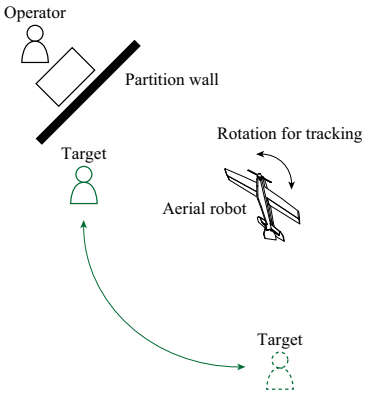

Fig. 14. Schematic view of target tracking teleoperation.

Therefore, automatic obstacle avoidance capability is very important. We developed the preliminary obstacle avoidance system. An extra ultrasonic sensor is mounted on the fuselage mid-section. When the distance between the UAV and obstacle d_o is less than the threshold (safety limit) d_{th}, the elevator angle is controlled by following simple PI controller:

$$\delta_2 = -\left(K_P(d_{th} - d_o) + K_I \int (d_{th} - d_o) dt \right) , \qquad (13)$$

where δ_2 is the elevator angle and d_{th} is 1.5 m. Fig. 17 shows the schematic view of obstacle avoidance.

One directional obstacle avoidance experiment was performed to verify the system. Fig. 18 shows the distance between the UAV and obstacle. Fig. 19 shows attitude change during the experiment. The snapshots of obstacle avoidance experiment are shown in Fig. 20. The operator commanded diagonally forward right velocity. When the ultrasonic sensor detected the front obstacle, the UAV ignored forward velocity command and moved rightward. Then, the UAV moved diagonally forward right again.

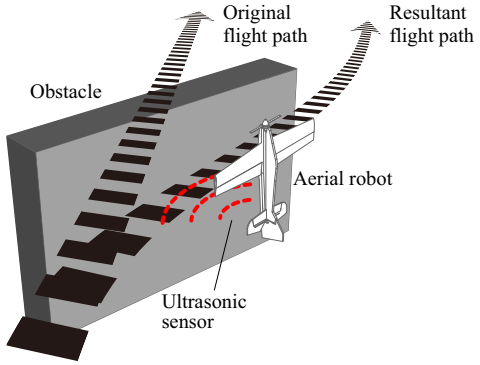

Fig. 17. Obstacle avoidance with ultrasonic sensor.

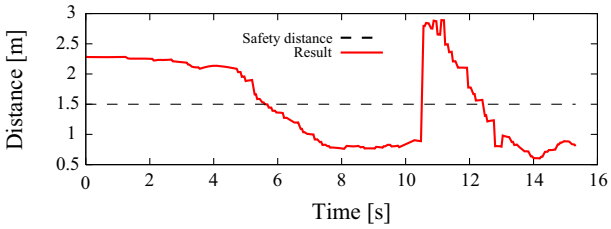

Fig. 18. Distance change between the UAV and the obstacle.

Fig. 15. Target tracking teleoperation.

Fig. 16. Target tracking teleoperation (fuselage mid-section camera).

Fig. 20. Obstacle avoidance experiment.

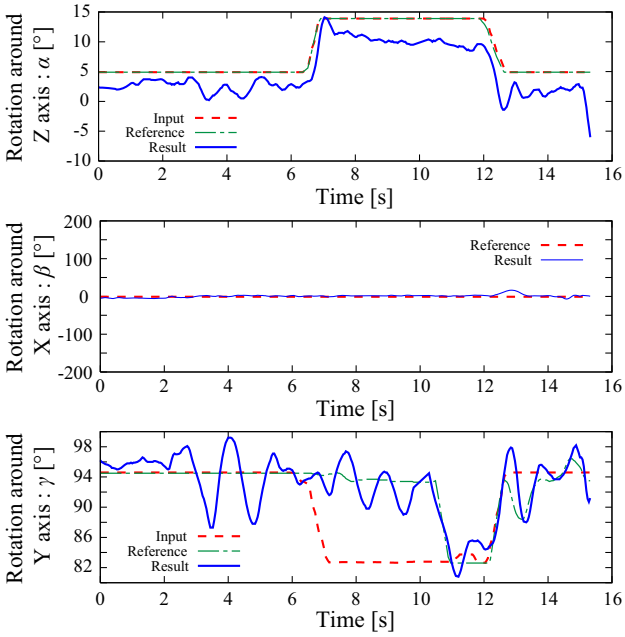

Fig. 19. Attitude change during obstacle avoidance experiment (α, β and γ are ZXY Euler angles, respectively).

V. CONCLUSIONS

In this paper, a teleoperation system is developed to navigate the tail-sitter VTOL UAV. Velocity control strategies for both outdoor and indoor teleoperated hovering exploration were presented. Utilizing teleoperation system and control strategy, the operator achieved indoor exploration experiment and target tracking teleoperation without the line-of-sight of the operator. In order to assist the operator to concentrate teleoperation, preliminary obstacle avoidance system was developed. The experiment result show that the proposed system worked successfully and the UAV avoided obstacle automatically. Because the purpose of this paper is practice of basic experiments, the UAV was equipped with minimum requested cameras and sensors; however, forward camera for level flight and upward distance sensor for vertical hover will be equipped in the furure.

REFERENCES

[1] R. Beard, D. Kingston, M. Quigley, D. Snyder, R. Christiansen, W. Johnson: "Autonomous Vehicle Technologies for Small Fixed-Wing UAVs," *J. of Aerospace Computing, Information and Communication*, Vol.2, pp. 92-108, January 2005.

[2] N. Guenhard, T. Hamel, L. Eck: "Control Laws for the Tele Operation of An Unmanned Aerial Vehicle Known As An X4-flyer," *in Proc. of the 2006 IEEE/RSJ Int. Conf. on Intelligent Robots and Systems*, Beijing, October 2006.

[3] R. H. Stone: "Control Architecture for a Tail-Sitter Unmanned Air Vehicle," *in Proc. of the 5th Asian Control Conference*, Vol. 2, pp. 736-744, 2004.

[4] W. E. Green, P. Y. Oh: "Autonomous Hovering of a Fixed-Wing Micro Air Vehicle," *in Proc. of the 2006 IEEE International Conference of Robotics and Automation*, 2006.

[5] W. E. Green, P. Y. Oh: "A MAV That Flies Like an Airplane and Hovers Like a Helicopter," *in Proc. of the 2005 IEEE/ASME Int. Conf. on Advanced Intelligent Mechatronics*, pp.693-698, 2005.

[6] K. Kita, A. Konno and M. Uchiyama: "Hovering Control of a Tail-Sitter VTOL Aerial Robot," *J. of Robotics and Mechatronics*, vol. 21, no. 2, pp. 277-283, 2009.

[7] K. Kita, A. Konno and M. Uchiyama: "Transitions Between Level-Flight and Hovering of a Tail-Sitter VTOL Aerial Robot," *Advanced Robotics*, vo. 24, no. 5-6, pp. 763-781, 2010.

[8] T. Matsumoto, K. Kita, R. Suzuki, A. Oosedo, K. Go, Y. Hoshino, A. Konno and M. Uchiyama: "A Hovering Control Strategy for a Tail-Sitter VTOL UAV that Increases Stability Against Large Disturbance," *in Proc. of the 2010 IEEE Int. Conf. of Robotics and Automation*, pp. 54-59, 2010.

[9] M. Naruoka and T. Tsuchiya: "A Powerful Autopilot System for Small UAVs with Accurate INS/GPS Integrated Navigation," *in Proc. of the 2007 JSASS-KSAS Joint Int. Symposium on Aerospace Engineering*, pp. 10-12, Kitakyushu, October, 2007.